The Excitation of Solar Oscillations
−−Observations and Simulations

Philip R. Goode

Big Bear Solar Observatory, New Jersey Institute of Technology, Big Bear City, CA 92314

Louis H. Strous

Big Bear Solar Observatory, New Jersey Institute of Technology, Big Bear City, CA 92314
Lockheed-Martin Solar & Astrophysics Lab, Palo Alto, CA 94304

Thomas R. Rimmele

National Solar Observatory, Sunspot, NM 88349

R. F. Stein

Department of Physics and Astronomy, Michigan State University, East Lansing, MI 48824

Å. Nordlund

Theoretical Astrophysics Center and Astronomical Observatory, Dk-2100 Copenhagen, Denmark

Abstract. We compare observations of the excitation of solar oscillations with simulations. We pass synthetic line profile data through the same analysis scheme used for observed line profiles. We find in both cases that seismic events exciting the oscillations are largely confined to the dark intergranular lanes. The excitation is closely associated with the collapse of the intergranular lanes, rather than the continuous drumming of turbulent convection. The most significant difference in the results is the considerably longer lifetime of the observed events.

1. Introduction

It has been known for many years that solar oscillations are excited very close to the Sun's surface [Goldreich and Keeley 1977, Goldreich and Kumar 1989]. Rimmele, et al. (1995) observed that seismic events originate in the dark intergranular lanes as a part of a cooling and collapse of the solar surface. Goode, et al. (1998) showed that the seismic events feed power into the Sun's normal modes.

The observations are photospheric line profile data covering a two dimensional field of view. By measuring the velocity as a function of depth in the line, we are able to determine velocity and phase information as a function of altitude. This three dimensional velocity information coupled with the vertical phase gradient is the key to identifying the kind of seismic events we study. There is power in two regions of our k-ω diagram. Our seismic events are in the p-mode region where these normal modes are evanescent. However, we observe there a second kind of acoustic signal−−*the seismic event*−−which is characterized by a sizeable vertical gradient, as though it were first travelling upwards. The last part of the event occurs a few minutes later. This part looks like a wave travelling back down in the same point in the field of view, as though it was reflected back down from above. This clear phase evolution, coupled with the spatial and temporal isolation of the events, enables us to distinguish the events from p-modes which have virtually no vertical phase gradient. It is these seismic events that Rimmele, et al. found populating the dark lanes. They also found the power in the events was sufficient to drive the entire p-mode spectrum.

The synthetic line profile data comes from the large scale simulations of the velocity field in the outer layers of the Sun due to Stein and Nordlund (1998). These calculated "data" match the cadence of the observations, and are passed through exactly the same redution scheme. The observations and data reduction are discussed in the next section.

Our pupose here is to compare and contrast seismic events from observations and simulations.

2. The Data and the Reduction of It

Our observations were made at the Vacuum Tower Telescope of the National Solar Observatory in Sunspot, New Mexico. The quiet Sun dataset discussed here is from Sept. 5, 1994. The data and the reduction of it are described in detail in Rimmele, et al. (1994, 1995), and references therein. One of the basic observational problems here is to distinguish the seismic event power from the dominant resonant mode power. To distinguish the two in our field of view ($60'' \times 60''$ patch of quiet Sun near disk center), Rimmele, et al. measured the velocity as a function of altitude in the photosphere for 65 min by observing the Doppler shift in the 543.4 nm Fe I absorption line. The Doppler shift as a function of depth in the line corresponds to the velocity as a function of altitude in the atmosphere the line spans.

We note that earlier spectrographic observations of the Fe I line, Stebbins and Goode (1987), but with a faster cadence and one dimensional field of view, the basic life cycle of the events was the same ours, see Restaino, et al. (1993). Also, observations measuring other lines show the same basic results for the events, e.g., the well-known Fe I 5576 Å (g=0) line.

In the data reduction, we calculate $v(x, y, z, t)$, the four dimensional velocity cube. In the z-direction, ten depths in the 543.4 nm line yield velocities at ten altitudes spanning the photosphere. From this, we determine we determine the seismic flux which is defined as

$$u \propto \frac{V^2}{\omega} \frac{\Delta\phi}{\Delta z},$$

where V is the local velocity amplitude and $\frac{\Delta\phi}{\Delta z}$ is the vertical phase gradient and

ω is the instantaneous oscillation frequency which is assumed to be constant. If the seismic flux were describing an acoustic travelling wave (above the acoustic cut-off), then the seismic flux would be identical to the ordinary mechanical flux. However, the seismic power is beneath the acoustic cut-off. Nonetheless, the seismic flux is a useful measure of the events and enables us to distinguish the events from p-modes. The k-ω diagram for the data is shown in Figure 1. The power is concentrated in two places−−the low frequency power arises from

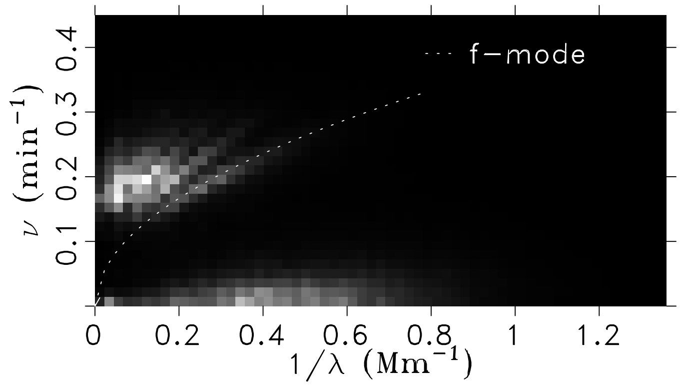

Figure 1. The k-ω diagram for the observational data. The dashed white curve represents the calculated f-mode ridge. Note that the sonic and subsonic regions are well separated. Note also that there is significant power in the region of the f-mode ridge.

the convective flows. In fact, if we filter to pass only that power, the velocity field from near the continuum looks the same as that from a second CCD we employed to simultaneously measure the white light. The remaining power is in the p-mode region which is, of course, below the acoustic cut-off. This power consists of seismic events and p-modes, as Rimmele, et al. emphasized. A typical event is characterized by a 30° or more phase change through the photosphere at some time in its life. The lifecycle of events is described in detail in Rimmele et al. and Goode et al..

3. Seismic Events

In Figure 2, we show a contoured scatter plot of the seismic flux against the local convective velocity for the velocity cube. The events shown are the upper 10% of the events, and as such represent more that 2000 events as identified in Goode, et al. (1998). There is a linear relation between the velocity and seismic flux given by Strous, Goode and Rimmele (1998)

$$\frac{v_{\rm down}}{\rm m/s} = (-0.115 \pm 0.003) - (0.012 \pm 0.002)\frac{F_{\rm ac}}{100{\rm kW/m^2}} \pm 0.060,$$

where $F_{\rm ac}$ is the seismic flux and $v_{\rm down}$ is the local convective velocity. This relationship says that the greater the downgoing convective velocity, the greater the seismic flux. More significantly is the linear relation itself would be unexpected if turbulent convection itself drove the oscillations. In that case, one would expect the event power to go as a high power of the convective velocity, Goldreich and Kumar (1990). We emphasize here that the observational data imply that the seismic events arise from cooling and collapse of the solar surface as a part of the convective overshooting, but not as the continuous drumming of the turbulent convection itself.

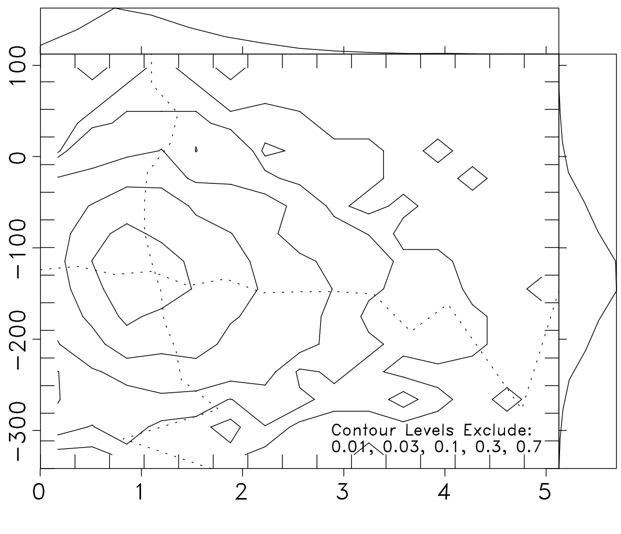

Figure 2. Extreme downward convective velocity vs. maximum seismic flux. A contour plot of the frequency distribution of the largest downward velocity (in m/s) versus the maximum seismic flux (in units of 100 kW/s) in all approximately 2000 seismic events. The contour levels indicate the fraction of data points that lies on the outside of the corresponding contour. For instance, the central contour excludes 70% of the data points. The small side panels show the associated one-dimensional frequency distributions.

In Figure 3, we show the time evolution of the averaged seismic events shown in Figure 2. The events are pinned in time with t=0 s being the peak of the upgoing flux for each. The flux is shown in the white contours. The events are overlayed on the local granular field, shown in grayscale. The field is oriented with the local lane along the x-axis and the brighter feature on top. Clearly the events originate in the intergranular lanes. This is a robust feature surviving the averaging of more than 2000 events, Goode, et al. (1998). If we examine the components of the seismic flux as they evolve from the center of the mean event (see Figure 2 of Goode, et al.), we find that there is an excess V^2 power that is apparent out to beyond $2''$ from the center of the event. On the other hand, the phase gradient shows ever diminishing event-like behavior (outgoing wave following by ingoing wave) which is absent beyond about $1''$ from the event center. Thus, beyond $1''$ the excess power shows essentially no vertical phase gradient, and, therefore, event power has changed form to look like normal mode power. In detail, this power looks like f-mode power as seen in Figure 1. Kumar (1993) has shown that one can expect seismic event power to be converted to p-mode power after a few subsurface skips. That is, their power would come to reside on the p-mode ridges of the k-ω diagram. However, the skip times and distances are so great that in a single skip a normal mode would be out of our field of view and its subsurface travel time would be longer than the temporal duration of our dataset. However, f-modes are, asymptotically, surface waves, so that their skip times and distances are small. Thus, these are the only normal modes we can expect to see resulting from the seismic events−−and we do see them. We also note that the V^2 power falls off as the distance squared, as one would anticipate. The averaged vertical phase gradient has a peak value of somewhat less than 3°. This value is so small because it arises from the averaging of many events. In fact this value is significant well above a 10σ level. Strous, Goode and Rimmele looked for seismic ripples beyond 4" from the center of the mean events. They found nothing that was inconsistent with noise.

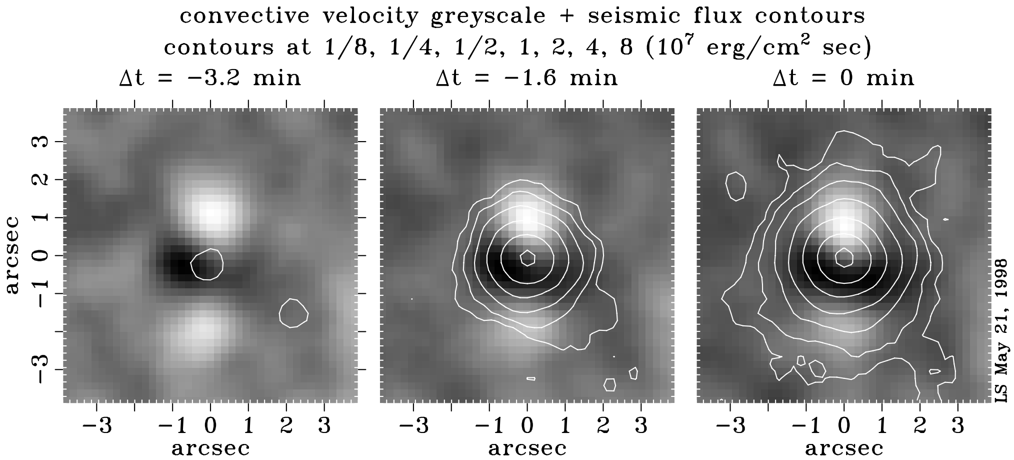

Figure 3. From observations: The superposed seismic flux, shown in white contours, is superposed on its local, averaged granulation altitude 150 km above the base of the photosphere. The contours are 0.25, 0.5, 1, 2, 4×10^7 ergs/cm^2/s. The time steps in the data collection are about 30 s, and at one time step before $T{=}{-}3.2$ min, the seismic flux is below 0.25×10^7 ergs/cm^2/s everywhere in the field of view.

In Figure 4, we show a scatter plot of the analyzed synthetic line profile data. This plot is meant to be compared to Figure 2. We see that the greater the downgoing convective velocity, the greater the local seismic event. Further, the relationship is linear, as in Figure 2.

In Figure 5, we see the k-ω diagrams from the synthetic line profile data. The plot on the right hand side of the figure is the k-ω diagram which has been

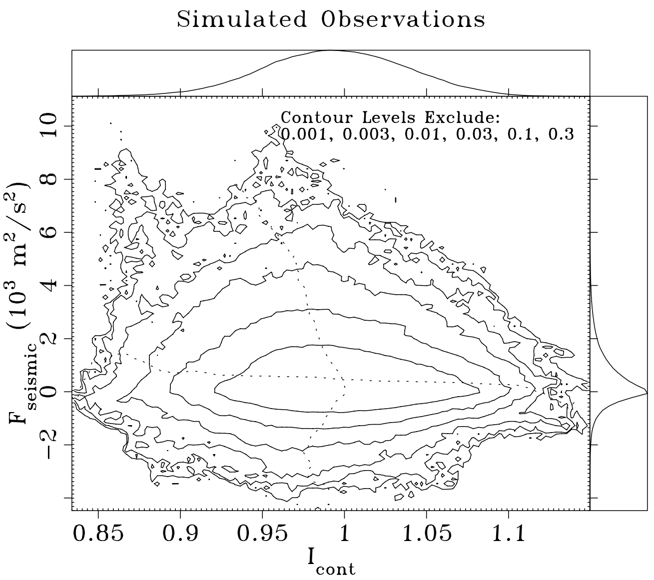

Figure 4. From simulations: The superposed seismic flux, shown in white contours, is superposed on its local, averaged granulation altitude 150 km above the base of the photosphere. The contours are 0.25, 0.5, 1, 2, 4×10^7 ergs/cm^2/s. The time steps in the data collection are about 30 s, and at one time step before T=-3.2 min, the seismic flux is below 0.25×10^7 ergs/cm^2/s everywhere in the field of view.

degraded to account for the effects of atmospheric turbulence. As in Figure 1, the power is confined to two regions of the diagram. When we filter either of these diagrams to pass only the low frequency or convective power, we obtain the granular field. When we pass the power for the higher frequency region, we have the p-mode power and the event power discussed here. Of course, we use the vertical phase gradient information to delineate between the latter two kinds of power. We note that there is also power with vertical phase gradients in the convective region. Much of this power is associated with granular evolution. In particular, if the edge of a granule moves across some point in the field of view, its horizontal motion, which is differential with altitude, may cause a signal which resembles a vertically propagating wave. Could there be seismic event power in the the convective region of the power spectrum? Well, if the spectrum of seismic events were to extend from the p-mode region to the convection region in the k-ω diagram, then we would expect event power in the convection region. However, there is no such connection between the regions.

In Figure 6, we show the simulated granulation and seismic flux at a particular, but typical instant−−both the results from the full velocity signal and that degraded in our effort to mimic the effects of seeing. The degraded signal looks quite like that from the observational data. It is clear that the seismic power lies in the intergranular lanes, just as was determined from the observations. Further, the events from the simulations do typically have the characteristic evolution of an upgoing event followed by a downgoing event. However, the downgoing flux in the latter stages of the events seems weak. This weakness is

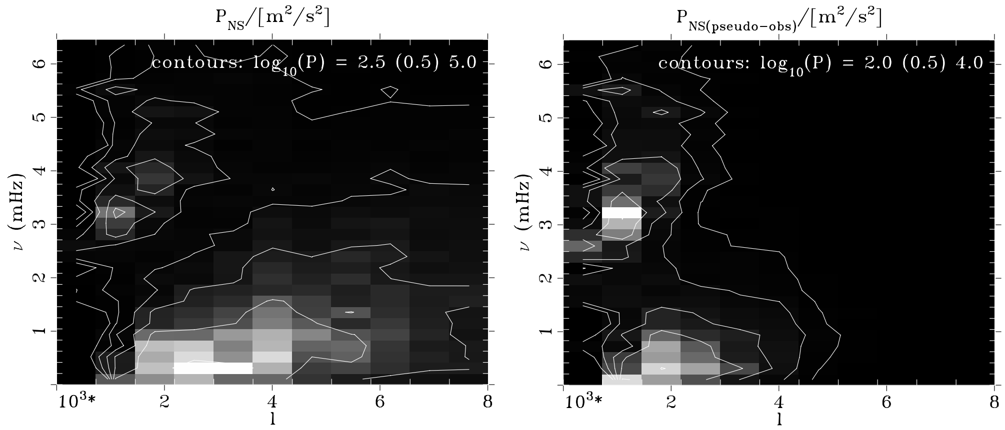

Figure 5. The k-ω diagrams for the simulations. The one on the right has the velocity signal degraded to account for seeing.

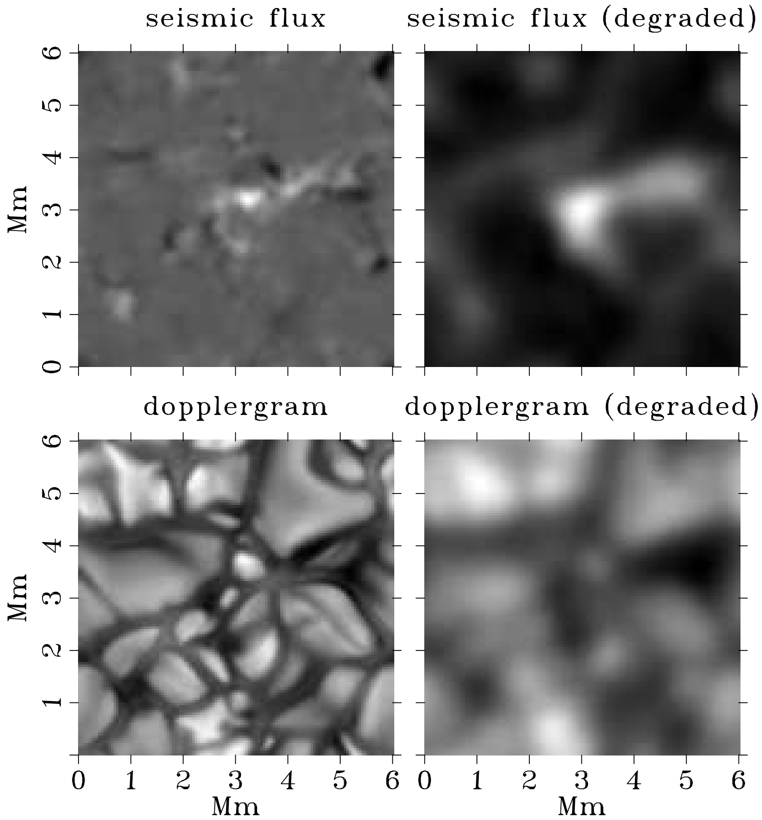

Figure 6. The left hand panels are a snapshot of the seismic flux and Doppler velocities for the full resolution simulations. Both the flux and granulation are shown in gray scale with bright meaning upgoing and dark meaning downgoing. On the right is the same snapshot in time, but with the velocity signal being degraded by seeing effects.

probably due to the fact that the outer boundary condition in the model is that all waves reaching the temperature minimum propagate out of the box. The full resolution image reveals the role of small, but not necessarily weak granules. The small bright granules in the center of the field of view are at the heart of the strongest seismic flux in the image. In the events, these small granules collapse and bring down part of the neighboring granule. We also see this in particular examples of the observed seismic events. However, there are real differences betweens the observed events and those from the simulations. Most striking is the fact that the real events last 2-3 times longer than the simulated ones. This fact and other significant results of the comparison are currently under study, Strous, et al. (1998).

We are investigating the seismic potential of the events. However, we know that the probing will be very local. That is, no seismic signal is detected beyond about 3-4$''$ away from the center of an event. We believe the seismic probing would be most effective in probing nearby granules. The seismology will be aided by our ablity to compare observed and simulated probings. We also will study the power of the events to probe small, weak magnetic features like pores.

P.R.G. and L.H.S. were supported in part by NSF-ATM-97-14796 and NAG5-4919. T.R.R. is supported by the National Solar Observatory which is operated by AURA under cooperative agreement with the National Science Foundation. R.F.S. was supported by NAG-1695, NAG5-4031 and NSF-AST-95-21785. Å.N. was supported in part by the Danish Research Foundation.

References

Goldreich, P. & Keeley, D.A., 1977, ApJ, 212, 243.

Goldreich, P. & Kumar, P., 1988, ApJ, 326, 462.

Goldreich, P. & Kumar, P., 1990, ApJ, 363, 694.

Goode, P.R., Strous, L.H., Rimmele, T.R.,& Stebbins, R.T., 1998, ApJ, 495, L27.

Kumar, P., 1993, in *GONG 1992: Seismic Investigation Of The Sun And Stars*, ed. T.M. Brown, A.S.P. Conf. Ser. 42, 15.

Restaino, S.R., Stebbins, R.T. & Goode, P.R., 1993, ApJ, 408, L57.

Rimmele, T.R., 1994, A&A, 290, 972.

Rimmele, T.R., Goode, P.R., Harold, E. and Stebbins, R.T., 1995, ApJ, 444, L119.

Stebbins, R.T. & Goode, P.R., 1987, Solar Phys., 110, 237.

Stein, R.F. & Nordlund, Å, 1998, ApJ, 499, 914.

Strous, L.H., Goode, P.R. & Rimmele, T.R., 1998, in preparation.

Strous, L.H., Goode, P.R., Rimmele, T.R., Nordlund, Å. & Stein, R.F., 1998, in preparation.